Energy Minimizing Spatial Cubic Geometric Hermite Interpolation Curve

Juncheng Li, and Chengzhi Liu

Abstract—**The energy minimization had been wieldy applied to select two free parameters of the planar cubic geometric Hermite interpolation curve. However, the energy minimization of the spatial cubic geometric Hermite interpolation curve seems to have been neglected. Since the spatial geometric Hermite interpolation curve has both bending and twisting, the bending energy and twisting energy should be simultaneously considered when selecting the two free parameters by energy minimization. This paper introduces the bending energy and the twisting energy of the spatial cubic geometric Hermite interpolation curve, and then presents the bending and twisting energy minimization method for selecting the two free parameters. The proposed minimization is achieved by solving a bi-objective optimization problem, and the unique approximate solution of the bi-objective optimization problem is given. Some numerical examples show that the proposed method makes the spatial cubic geometric Hermite interpolation curve have the minimum bending energy as well as the minimum twisting energy.**

Index Terms—**Hermite interpolation, spatial curve, bending energy, twisting energy, minimization**

I. INTRODUCTION

The cubic geometric Hermite interpolation curve (CGHI-curve for short) can be described by the Bézier form as follows [1],

$$\begin{aligned}\boldsymbol{b}(t) = \boldsymbol{p}_0 B_0^3(t) + (\boldsymbol{p}_0 + \frac{1}{3}\alpha_0 \boldsymbol{d}_0) B_1^3(t) + \\ (\boldsymbol{p}_1 - \frac{1}{3}\alpha_1 \boldsymbol{d}_1) B_2^3(t) + \boldsymbol{p}_1 B_3^3(t),\end{aligned} \tag{1}$$

where $B_k^3(t) = \dfrac{3!}{k!(3-k)!} t^k (1-t)^{3-k}$ $(k = 0,1,2,3)$, $\boldsymbol{p}_0, \boldsymbol{p}_1$ are two points, $\boldsymbol{d}_0, \boldsymbol{d}_1$ are unit tangent directions at the two points, and α_0, α_1 are two positive numbers. The two points and the associated tangent directions are usually given in practical application, but the two positive numbers are often used as free parameters.

Recently, curves with free parameters have been widely concerned (see [2-7]). In like wise, the CGHI-curve has two free parameters when the two points and the associated unit tangent directions are fixed. Hence, many researchers selected the two free parameters of planar CGHI-curve by minimizing the bending energy (also known as strain energy) or the curvature variation energy (see [8-15]). However, how to use energy minimization to select the two free parameters of spatial CGHI-curve seems to have been neglected.

As we know, planar curves only need to consider bending, while spatial curves should consider not only bending but also twisting. Although the energy minimization for Hermite curve in R^d was presented in [16], they only used the bending of the curve. The bending and twisting minimization for 3D curves were addressed in [17], but the method is framed in terms of B-spline curves. A natural problem arises: how to select the two free parameters of the spatial CGHI-curve by minimizing both bending energy and twisting energy. This paper first proposes the bending energy and the twisting energy of the spatial CGHI-curve, and then presents the bending and twisting energy minimization for selecting the two free parameters of the curve.

The rest of this paper is organized as follows. In Section II the bending energy and the twisting energy of the spatial CGHI-curve are introduced. In Section III the bending and twisting energy minimization is described. In Section IV some numerical examples are shown. Finally, a short conclusion is given in Section V.

II. ENERGY OF THE SPATIAL CGHI-CURVE

For the spatial CGHI-curve $\boldsymbol{b}(t)$ $(0 \le t \le 1)$, the bending energy and the twisting energy of the curve can be described by (see [17])

$$E_{\text{bend}} = \int_0^1 \kappa^2(t) \|\boldsymbol{b}'(t)\| \mathrm{d}t, \tag{2}$$

$$E_{\text{twist}} = \int_0^1 \tau^2(t) \|\boldsymbol{b}'(t)\| \mathrm{d}t, \tag{3}$$

where $\kappa(t)$ and $\tau(t)$ represent the curvature and the torsion of the curve respectively, and

$$\kappa(t) = \frac{\|\boldsymbol{b}'(t) \times \boldsymbol{b}''(t)\|}{\|\boldsymbol{b}'(t)\|^3},\ \tau(t) = \frac{(\boldsymbol{b}'(t), \boldsymbol{b}''(t), \boldsymbol{b}'''(t))}{\|\boldsymbol{b}'(t) \times \boldsymbol{b}''(t)\|^2}.$$

In order to facilitate the calculation, the bending energy (2) and the twisting energy (3) could be approximately described by (see [17])

Manuscript received July 20, 2021; revised October 27, 2021. This work was supported by the Hunan Provincial Natural Science Foundation of China under Grant No. 2021JJ30373, and the National Natural Science Foundation of China under Grant No. 12101225.

Juncheng Li is a professor of College of Mathematics and Finance, Hunan University of Humanities, Science and Technology, Loudi 417000, PR China (corresponding author phone: +86 738 8325585; fax: +86 738 8325585; e-mail: lijuncheng82@126.com).

Chengzhi Liu is an associate professor of College of Mathematics and Finance, Hunan University of Humanities, Science and Technology, Loudi 417000, PR China (e-mail: it-rocket@163.com).

$$\hat{E}_1 = \int_0^1 \|\boldsymbol{b}''(t)\|^2 \mathrm{d}t , \tag{4}$$

$$\hat{E}_2 = \int_0^1 \|\boldsymbol{b}'''(t)\|^2 \mathrm{d}t . \tag{5}$$

Here, the approximate expressions (4) and (5) are adopted to describe the bending energy and the twisting energy of the spatial CGHI-curve.

It should be noted that (4) was regarded as an approximate bending energy of the planar CGHI-curve in [8, 9], and (5) was regarded as an approximate curvature variation energy of the planar CGHI-curve in [12].

III. Energy minimization of the spatial CGHI-curve

By a deduction from (1), then

$$\boldsymbol{b}''(t) = 2\alpha_0(-2+3t)\boldsymbol{d}_0 - 2\alpha_1(1-3t)\boldsymbol{d}_1 + 6(1-2t)\Delta\boldsymbol{p}_0 , \tag{6}$$

$$\boldsymbol{b}'''(t) = 6(\alpha_0\boldsymbol{d}_0 + \alpha_1\boldsymbol{d}_1 - 2\Delta\boldsymbol{p}_0) , \tag{7}$$

where $\Delta\boldsymbol{p}_0 := \boldsymbol{p}_1 - \boldsymbol{p}_0$. Let $\theta_0 := \angle(\boldsymbol{d}_0, \Delta\boldsymbol{p}_0)$, $\theta_1 := \angle(\boldsymbol{d}_1, \Delta\boldsymbol{p}_0)$, $\theta_2 := \angle(\boldsymbol{d}_0, \boldsymbol{d}_1)$, where $\angle(\boldsymbol{a}, \boldsymbol{b})$ represents the angle between $\boldsymbol{a}$ and $\boldsymbol{b}$. Here $0 \le \angle(\boldsymbol{a}, \boldsymbol{b}) \le \pi$.

By computing from (4) and (6), the approximate bending energy functional of $\boldsymbol{b}(t)$ becomes

$$\begin{aligned}\hat{E}_1(\alpha_0,\alpha_1) = 4\big(&\alpha_0^2 + \alpha_1^2 + \alpha_0\alpha_1\cos\theta_2 - 3\alpha_0\|\Delta\boldsymbol{p}_0\|\cos\theta_0 \\ &-3\alpha_1\|\Delta\boldsymbol{p}_0\|\cos\theta_1 + 3\|\Delta\boldsymbol{p}_0\|^2\big).\end{aligned} \tag{8}$$

By computing from (5) and (7), the approximate twisting energy functional of $\boldsymbol{b}(t)$ becomes

$$\begin{aligned}\hat{E}_2(\alpha_0,\alpha_1) = 36\big(&\alpha_0^2 + \alpha_1^2 + 2\alpha_0\alpha_1\cos\theta_2 - 4\alpha_0\|\Delta\boldsymbol{p}_0\|\cos\theta_0 - \\ &4\alpha_1\|\Delta\boldsymbol{p}_0\|\cos\theta_1 + 4\|\Delta\boldsymbol{p}_0\|^2\big).\end{aligned} \tag{9}$$

Here, since both the bending energy and the twisting energy need be minimized and a feasible region

$$D := \{(\alpha_0,\alpha_1) \in \mathrm{R}^2 \,|\, \alpha_0 > 0, \alpha_1 > 0\}$$

should be applied, then the following bi-objective problem would need to be solved,

$$\min_{(\alpha_0,\alpha_1)\in D} \left(\hat{E}_1(\alpha_0,\alpha_1), \hat{E}_2(\alpha_0,\alpha_1)\right)^{\mathrm{T}} . \tag{10}$$

The bi-objective problem (10) could be transformed into

$$\min_{(\alpha_0,\alpha_1)\in D} \hat{E}(\alpha_0,\alpha_1,\lambda) = \lambda\hat{E}_1(\alpha_0,\alpha_1) + (1-\lambda)\hat{E}_2(\alpha_0,\alpha_1) , \tag{11}$$

where λ $(0 \le \lambda \le 1)$ is the weight.

Before solving problem (11), the value of the weight λ needs to be selected. For this purpose, the bending energy minimization and the twisting energy minimization of the spatial CGHI-curve are first introduced.

In [8, 9], (4) was regarded as an approximate bending energy of the planar CGHI-curve and the corresponding bending energy minimization was addressed. Since we use (4) as an approximate bending energy of the spatial CGHI-curve, the corresponding bending energy minimization could be described by the following theorem with reference to the experience in [8, 9].

Theorem 1. *The approximate bending energy functional* $\hat{E}_1(\alpha_0,\alpha_1)$ *has a unique global minimum. And the minimum, set as* $(\alpha_0^{(1)},\alpha_1^{(1)})$ *, is expressed as*

$$\alpha_0^{(1)} = \frac{3\|\Delta\boldsymbol{p}_0\|(2\cos\theta_0 - \cos\theta_1\cos\theta_2)}{4-\cos^2\theta_2} , \tag{12}$$

$$\alpha_1^{(1)} = \frac{3\|\Delta\boldsymbol{p}_0\|(2\cos\theta_1 - \cos\theta_0\cos\theta_2)}{4-\cos^2\theta_2} . \tag{13}$$

Furthermore, the minimum lies in D if and only if

$$\begin{cases} 2\cos\theta_0 - \cos\theta_1\cos\theta_2 > 0, \\ 2\cos\theta_1 - \cos\theta_0\cos\theta_2 > 0. \end{cases} \tag{14}$$

Proof. By computing from (8), the gradients of $\hat{E}_1(\alpha_0,\alpha_1)$ can be calculated by

$$\frac{\partial\hat{E}_1}{\partial\alpha_0} = 4(2\alpha_0 + \alpha_1\cos\theta_2 - 3\|\Delta\boldsymbol{p}_0\|\cos\theta_0) ,$$

$$\frac{\partial\hat{E}_1}{\partial\alpha_1} = 4(2\alpha_1 + \alpha_0\cos\theta_2 - 3\|\Delta\boldsymbol{p}_0\|\cos\theta_1) .$$

The Hessian matrix of $\hat{E}_1(\alpha_0,\alpha_1)$ is given by

$$H_1 = 4\begin{pmatrix} 2 & \cos\theta_2 \\ \cos\theta_2 & 2 \end{pmatrix} .$$

It is easy to see that the matrix H_1 is symmetric positive definite. That means $\hat{E}_1(\alpha_0,\alpha_1)$ is strictly convex, and it has a unique global minimum. Then the unique minimum of $\hat{E}_1(\alpha_0,\alpha_1)$ expressed in (12) and (13) can be obtained by solving $\partial\hat{E}_1/\partial\alpha_0 = 0$ and $\partial\hat{E}_1/\partial\alpha_1 = 0$. If and only if (14) is satisfied, $\alpha_0^{(1)} > 0$ and $\alpha_1^{(1)} > 0$ are true. Thus the theorem has been proved.

In [12], (5) was regarded as an approximate curvature variation energy of the planar CGHI-curve and the corresponding curvature variation energy minimization had been addressed. Here, we use (5) as an approximate twisting energy of the spatial CGHI-curve. Drawing on the experience from [12], the twisting energy minimization of the spatial CGHI-curve could be described by the following theorem.

Theorem 2. *The approximate twisting energy functional* $\hat{E}_2(\alpha_0,\alpha_1)$ *has a unique global minimum as long as* $0 < \theta_2 < \pi$ *. And the minimum, set as* $(\alpha_0^{(2)},\alpha_1^{(2)})$ *, is expressed as*

$$\alpha_0^{(2)} = \frac{2\|\Delta\boldsymbol{p}_0\|(\cos\theta_0 - \cos\theta_1\cos\theta_2)}{1-\cos^2\theta_2} , \tag{15}$$

$$\alpha_1^{(2)} = \frac{2\|\Delta \boldsymbol{p}_0\|(\cos\theta_1 - \cos\theta_0\cos\theta_2)}{1-\cos^2\theta_2}. \quad (16)$$

Furthermore, the minimum lies in D if and only if

$$\begin{cases}\cos\theta_0 - \cos\theta_1\cos\theta_2 > 0,\\ \cos\theta_1 - \cos\theta_0\cos\theta_2 > 0.\end{cases} \quad (17)$$

Proof. By computing from (9), the gradients of $\hat{E}_2(\alpha_0,\alpha_1)$ can be calculated by

$$\frac{\partial \hat{E}_2}{\partial \alpha_0} = 72\left(\alpha_0 + \alpha_1\cos\theta_2 - 2\|\Delta\boldsymbol{p}_0\|\cos\theta_0\right),$$

$$\frac{\partial \hat{E}_2}{\partial \alpha_1} = 72\left(\alpha_1 + \alpha_0\cos\theta_2 - 2\|\Delta\boldsymbol{p}_0\|\cos\theta_1\right).$$

The Hessian matrix of $\hat{E}_2(\alpha_0,\alpha_1)$ is given by

$$H_2 = 72\begin{pmatrix} 1 & \cos\theta_2 \\ \cos\theta_2 & 1\end{pmatrix}.$$

It is easy to see that the matrix H_2 is symmetric positive definite as long as $0<\theta_2<\pi$. That means $\hat{E}_2(\alpha_0,\alpha_1)$ is strictly convex, and it has a unique global minimum. Then the unique minimum of $\hat{E}_2(\alpha_0,\alpha_1)$ expressed in (15) and (16) can be obtained by solving $\partial\hat{E}_2/\partial\alpha_0 = 0$ and $\partial\hat{E}_2/\partial\alpha_1 = 0$. If and only if (17) is satisfied, $\alpha_0^{(2)}>0$ and $\alpha_1^{(2)}>0$ are true. Thus the theorem has been proved.

To make sure that both $\left(\alpha_0^{(1)},\alpha_1^{(1)}\right)$ and $\left(\alpha_0^{(2)},\alpha_1^{(2)}\right)$ are available and that they lies in *D*, assume that

$$\begin{cases}0<\theta_0,\theta_1<\pi/2,\\ 0<\theta_2<\pi,\\ \cos\theta_0 > \cos\theta_1\cos\theta_2,\\ \cos\theta_1 > \cos\theta_0\cos\theta_2.\end{cases} \quad (18)$$

Then the value of the weight λ could be selected by using the ranking algorithm (see [18]) described as follows,

Step 1. Compute the deviations between the two objectives

$$\delta_i^{(j)} := \hat{E}_i(\alpha_0^{(j)},\alpha_1^{(j)}) - \hat{E}_i(\alpha_0^{(i)},\alpha_1^{(i)}),\ i,j=1,2.$$

Step 2. Compute the sum of the deviations of the two objectives $m_i := \sum_{j=1}^{2}\delta_i^{(j)}$, $i=1,2$.

Step 3. Compute the initial weights of the two objectives

$$\lambda_i := m_i/(m_1+m_2),\ i=1,2.$$

Step 4. If $m_1 \ge m_2$, set $\lambda = \min\{\lambda_1,\lambda_2\}$; else, set $\lambda = \max\{\lambda_1,\lambda_2\}$.

After selecting the value of the weight λ, the remaining task is to solve problem (11). The gradients of $\hat{E}(\alpha_0,\alpha_1)$ can be calculated by

$$\frac{\partial \hat{E}}{\partial \alpha_0} = 4\big((18-16\lambda)\alpha_0 + (18-17\lambda)\alpha_1\cos\theta_2 - (36-33\lambda)\|\Delta\boldsymbol{p}_0\|\cos\theta_0\big),$$

$$\frac{\partial \hat{E}}{\partial \alpha_1} = 4\big((18-17\lambda)\alpha_0\cos\theta_2 + (18-16\lambda)\alpha_1 - (36-33\lambda)\|\Delta\boldsymbol{p}_0\|\cos\theta_1\big).$$

The Hessian matrix of $\hat{E}(\alpha_0,\alpha_1)$ is given by

$$H = 4\begin{pmatrix} 18-16\lambda & (18-17\lambda)\cos\theta_2 \\ (18-17\lambda)\cos\theta_2 & 18-16\lambda\end{pmatrix}.$$

Because $-1\le\cos\theta_2\le 1$, $0\le\lambda\le 1$, then $18-16\lambda>0$ and

$$\begin{aligned}\det(H) &= 4\left((18-16\lambda)^2 - (18-17\lambda)^2\cos^2\theta_2\right)\\ &\ge 4\left((18-16\lambda)^2-(18-17\lambda)^2\right)\\ &>0.\end{aligned}$$

Thus the matrix H is symmetric positive definite. That means $\hat{E}(\alpha_0,\alpha_1)$ is strictly convex, and it has a unique global minimum which can be solved by $\partial\hat{E}/\partial\alpha_0 = 0$ and $\partial\hat{E}/\partial\alpha_1$. Then the global minimum of $\hat{E}(\alpha_0,\alpha_1)$ can be obtained as follows,

$$\alpha_0 = \frac{(36-33\lambda)\|\Delta\boldsymbol{p}_0\|((18-16\lambda)\cos\theta_0 - (18-17\lambda)\cos\theta_1\cos\theta_2)}{(18-16\lambda)^2-(18-17\lambda)^2\cos^2\theta_2}, \quad (19)$$

$$\alpha_1 = \frac{(36-33\lambda)\|\Delta\boldsymbol{p}_0\|((18-16\lambda)\cos\theta_1 - (18-17\lambda)\cos\theta_0\cos\theta_2)}{(18-16\lambda)^2-(18-17\lambda)^2\cos^2\theta_2}. \quad (20)$$

From (18), then

$$\begin{aligned}&(18-16\lambda)\cos\theta_0 - (18-17\lambda)\cos\theta_1\cos\theta_2\\ &=16(1-\lambda)(\cos\theta_0-\cos\theta_1\cos\theta_2) + 2(\cos\theta_0-\cos\theta_1\cos\theta_2)\\ &\quad +\lambda\cos\theta_1\cos\theta_2\\ &>2(\cos\theta_0-\cos\theta_1\cos\theta_2)+\lambda\cos\theta_1\cos\theta_2\\ &>\lambda(\cos\theta_0-\cos\theta_1\cos\theta_2)+\lambda\cos\theta_1\cos\theta_2\\ &=\lambda\cos\theta_0>0.\end{aligned}$$

That means α_0 expressed in (19) is positive. Similarly, α_1 expressed in (20) can also be verified to be positive. Thus the following theorem has been proved.

Theorem 3. *When (18) is satisfied, problem (11) has a unique approximate solution which reaches at (19) and (20).*

IV. Numerical Examples

In this section, the bi-objective energy minimization (*i.e.* the bending and twisting energy minimization) is compared with the bending energy minimization and the twisting energy minimization through some numerical examples.

Assume that

$$\boldsymbol{p}_0 = (0,0,0),\ \boldsymbol{p}_1 = (1,0,0),$$

$$\boldsymbol{d}_0 = (\cos\theta_0, \sin\theta_0\cos\alpha, \sin\theta_0\sin\alpha),$$

$$\boldsymbol{d}_1 = (\cos\theta_1, \sin\theta_1\cos\beta, \sin\theta_1\sin\beta),$$

and θ_0 , θ_1 , α , β are appropriately set so that (18) can be satisfied. It implies

$$\|\boldsymbol{d}_0\| = \|\boldsymbol{d}_1\| = 1,\ \angle(\boldsymbol{d}_0,\Delta\boldsymbol{p}_0) = \theta_0,\ \angle(\boldsymbol{d}_1,\Delta\boldsymbol{p}_0)=\theta_1.$$

The spatial CGHI-curves generated by three minimizations of four examples are illustrated in Fig. 1, where the viewing angle of the curves in (a) and (b) is azimuth=120°, elevation=60°, the viewing angle of the Hermite curves in (c) and (d) is azimuth=80°, elevation=20°.

The computational results of the four examples could be seen in Table I.

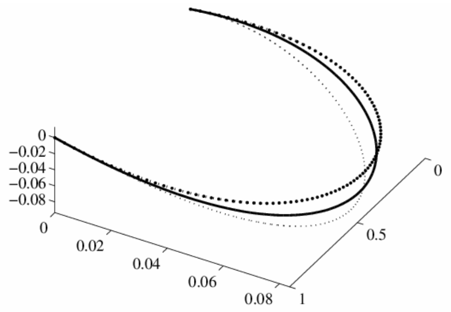

(a) $\theta_0 = \pi/3$, $\theta_1 = \pi/6$, $\alpha = \pi/6$, $\beta = 2\pi/3$

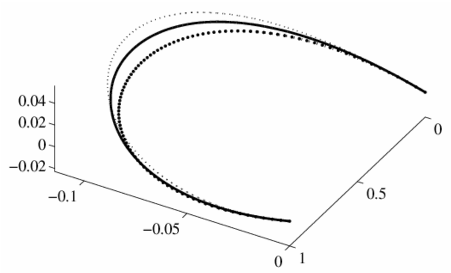

(b) $\theta_0 = \pi/6$, $\theta_1 = \pi/4$, $\alpha = 3\pi/4$, $\beta = \pi/6$

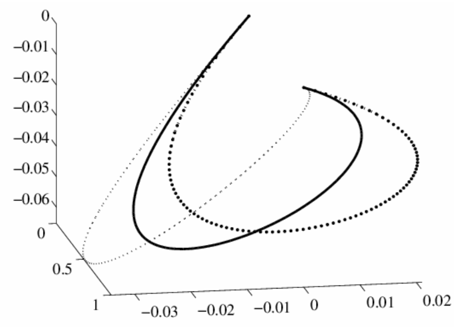

(c) $\theta_0 = \pi/12$, $\theta_1 = 2\pi/5$, $\alpha = 4\pi/3$, $\beta = 5\pi/6$

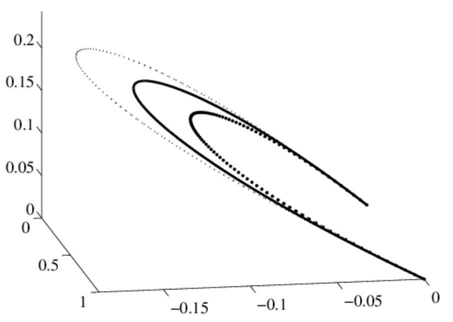

(d) $\theta_0 = \pi/4$, $\theta_1 = \pi/3$, $\alpha = 2\pi/3$, $\beta = 7\pi/4$

Fig. 1. Comparison of the bending energy minimization (thick dotted lines), the twisting energy minimization (thin dotted lines) and the bi-objective energy minimization (solid lines).

TABLE I.
THE COMPUTATIONAL RESULTS

Fig.1	Bending energy minimization		Twisting energy minimization		Bi-objective energy minimization	
	$\hat{E}_1$	$\hat{E}_2$	$\hat{E}_1$	$\hat{E}_2$	$\hat{E}_1$	$\hat{E}_2$
(a)	4.3	38.1	5.0	33.2	4.5	34.4
(b)	3.0	25.1	3.3	23.0	3.1	23.6
(c)	3.4	18.1	4.4	9.6	3.6	11.7
(d)	4.4	20.9	6.6	3.8	4.9	8.1

Table I shows that the bending energy and the twisting of the spatial CGHI-curve obtained by the bi-objective energy minimization are between those obtained by the other two energy minimizations. This means the spatial CGHI-curve generated by the bi-objective energy minimization has the minimum bending energy and the minimum twisting energy at the same time as far as possible, which is in line with the characteristic that both bending and twisting should be considered in spatial CGHI-curve.

The corresponding curvature plots and torsion plots of four examples are illustrated in Fig. 2 and Fig. 3 respectively.

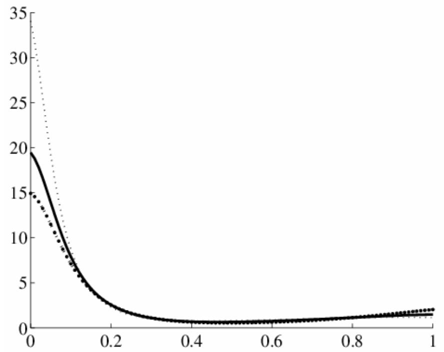

(a) $\theta_0 = \pi/3$, $\theta_1 = \pi/6$, $\alpha = \pi/6$, $\beta = 2\pi/3$

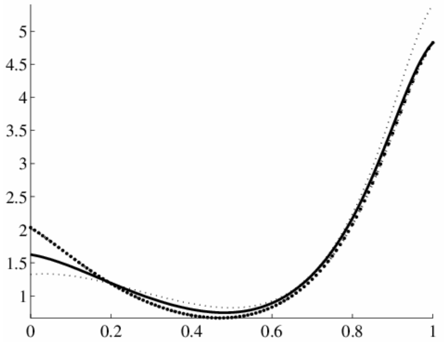

(b) $\theta_0 = \pi/6$, $\theta_1 = \pi/4$, $\alpha = 3\pi/4$, $\beta = \pi/6$

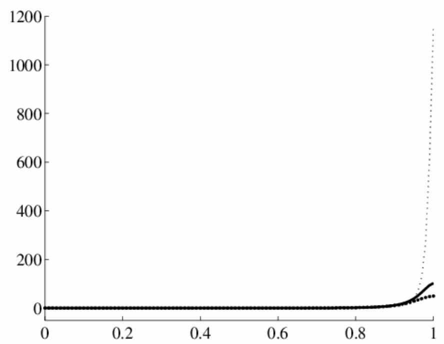

(c) $\theta_0 = \pi/12$, $\theta_1 = 2\pi/5$, $\alpha = 4\pi/3$, $\beta = 5\pi/6$

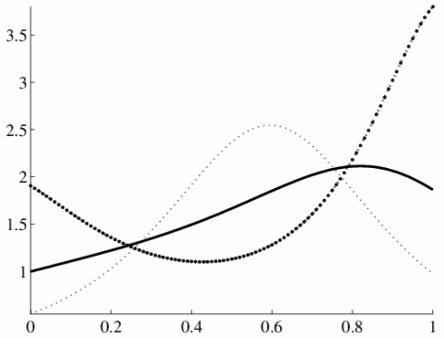

(d) $\theta_0 = \pi/4$, $\theta_1 = \pi/3$, $\alpha = 2\pi/3$, $\beta = 7\pi/4$

Fig. 2. Comparison of the curvature plots of the bending energy minimization (thick dotted lines), the twisting energy minimization (thin dotted lines) and the bi-objective energy minimization (solid lines).

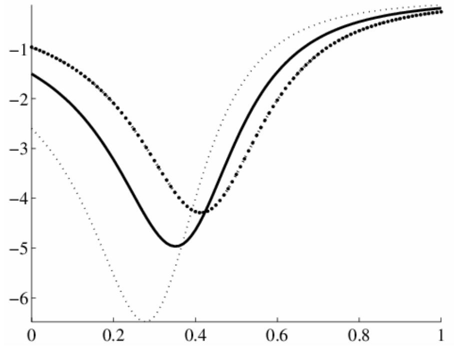

(a) $\theta_0 = \pi/3$, $\theta_1 = \pi/6$, $\alpha = \pi/6$, $\beta = 2\pi/3$

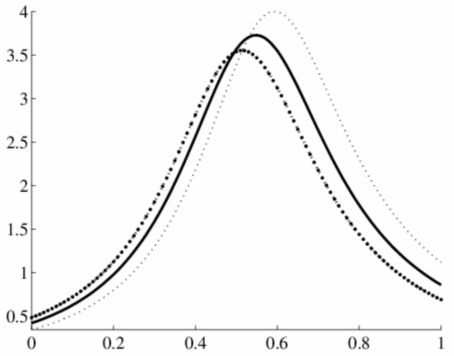

(b) $\theta_0 = \pi/6$, $\theta_1 = \pi/4$, $\alpha = 3\pi/4$, $\beta = \pi/6$

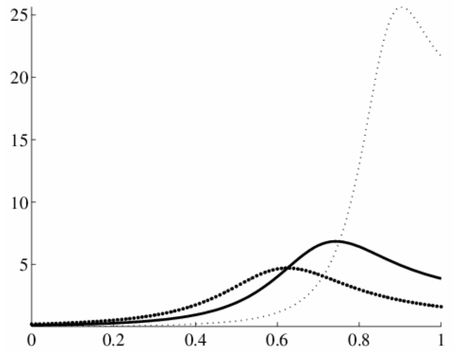

(c) $\theta_0 = \pi/12$, $\theta_1 = 2\pi/5$, $\alpha = 4\pi/3$, $\beta = 5\pi/6$

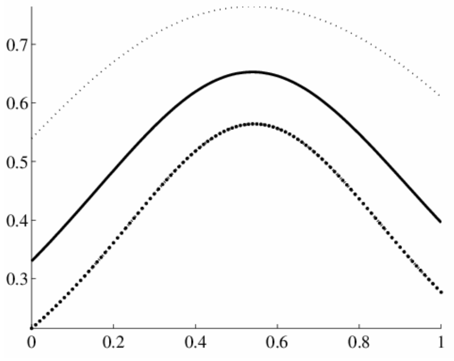

(d) $\theta_0 = \pi/4$, $\theta_1 = \pi/3$, $\alpha = 2\pi/3$, $\beta = 7\pi/4$

Fig. 3. Comparison of the torsion plots of the bending energy minimization (thick dotted lines), the twisting energy minimization (thin dotted lines) and the bi-objective energy minimization (solid lines).

Fig. 2 and Fig. 3 show that the curvature and the torsion of the spatial CGHI-curve obtained by the bi-objective energy minimization are between those obtained by the other two energy minimizations. This also verifies that the bi-objective energy minimization considers both bending and twisting of the spatial CGHI-curve, which is incomparable to the other two energy minimizations.

V. Conclusion

In this paper, how to select the two free parameters of the spatial CGHI-curve by minimizing both the bending energy and the twisting energy is presented. The curve obtained by the bi-objective energy minimization has less bending energy in the case of less twisting energy, which is verified through some numerical examples. The proposed method accords with the characteristic that both bending and twisting should be considered in spatial CGHI-curve. It is easy to find that the proposed method can be applied to select the free parameters of other spatial curves.

References

[1] G. Farin, *Curves and Surfaces for CAGD: a practical guide*. San Diego: Academic Press, 2002.

[2] L. L. Yan and J. F. Liang, “An extension of the Bézier model”, *Applied Mathematics and Computation*, vol. 218, no. 6, pp. 2863-2879, 2011.

[3] X. L. Han and Y. P. Zhu, “Curve construction based on five trigonometric blending functions”, *BIT Numerical Mathematics*, vol. 52, no. 4, pp. 953-979, 2012.

[4] X. Q. Qin, G. Hu, N. J. Zhang, X. L. Shen and Y. Yang, “A novel extension to the polynomial basis functions describing Bézier curves and surfaces of degree *n* with multiple shape parameters”, *Applied Mathematics and Computation*, vol. 223, pp. 1-16, 2013.

[5] X. B. Qin and Q. S. Xu, “C^1 positivity-preserving interpolation schemes with local free parameters”, *IAENG International Journal of Computer Science*, vol. 43, no. 2, pp. 219-227, 2016.

[6] L. Y. Peng and Y. P. Zhu, “A class of trigonometric Bézier basis functions with six shape parameters over triangular domain”, *IAENG International Journal of Applied Mathematics*, vol. 49, no. 4, pp. 618-624, 2019.

[7] J. C. Li and C. Z. Liu, " A class of polynomial spline curve with free parameters that naturally interpolates the data points", *IAENG International Journal of Applied Mathematics*, vol. 50, no. 3, pp. 643-647, 2020.

[8] J. H. Yong and F. Cheng, "Geometric Hermite curves with minimum strain energy", *Computer Aided Geometric Design*, vol. 21, no. 3, pp. 281-301, 2004.

[9] G. Jaklič and E. Žagar, "Planar cubic G^1 interpolatory splines with small strain energy", *Journal of Computational and Applied Mathematics*, vol. 235, no. 8, pp. 2758–2765, 2011.

[10] G. Jaklič and E. Žagar, "Curvature variation minimizing cubic Hermite interpolants", *Applied Mathematics and Computation*, vol. 218, no. 7, pp. 3918–3924, 2011.

[11] P. P. Li, C. M. Zhang, X. M. Li and W. T. Li, "Discussion on minimal curvature variation in cubic Hermite curve construction", *Journal of Advanced Mechanical Design, Systems, and Manufacturing*, vol. 6, no. 3, pp. 366-375, 2012.

[12] L. Z. Lu, "A note on curvature variation minimizing cubic Hermite interpolants", *Applied Mathematics and Computation*, vol. 259, pp. 596–599, 2015.

[13] L. Z. Lu, C. K. Jiang and Q. Q. Hu, "Planar cubic G^1 and quintic G^2 Hermite interpolations via curvature variation minimization", *Computer & Graphics*, vol. 70, pp. 92-98, 2017.

[14] J. C. Li and L. Zhang, "Length and curvature variation energy minimizing planar cubic G^1 Hermite interpolation curve", *Journal of Taibah University for Science*, vol. 14, pp. 60-64, 2020.

[15] J. C. Li, "Combined internal energy minimizing planar cubic Hermite curve", *Journal of Advanced Mechanical Design, Systems, and Manufacturing*, vol. 7, 2020.

[16] G. Jaklič and T. Kanduč, "Hermite and Lagrange interpolation in R^d by G^1 cubic splines with small strain energy", *Journal of Numerical Mathematics*, vol. 23, no. 3, pp. 257-270, 2015.

[17] R. C. Veltkamp and W. Wesselink, "Modeling 3D curves of minimal energy", In *Eurographics 95*, Maastricht, 1995, pp. 97–110.

[18] C. Y. Lin and J. L. Dong, "*The Methods and Theories of Multi-objective Optimizations*", Changchun: Jilin Education Press, 1992. (in Chinese)